

# Supporting Information:

## Singlet-Fission in TIPS-Anthracene Thin Films

Damon M. de Clercq,<sup>†</sup> Miles I. Collins,<sup>‡</sup> Nicholas P. Sloane,<sup>‡</sup> Jiale Feng,<sup>†</sup>  
Dane R. McCamey,<sup>‡</sup> Murad J. Y. Tayebjee,<sup>¶</sup> Michael P. Nielsen,<sup>¶</sup> and  
Timothy W. Schmidt<sup>\*,†</sup>

<sup>†</sup>*ARC Centre of Excellence in Exciton Science, School of Chemistry, UNSW Sydney, NSW 2052, Australia*

<sup>‡</sup>*ARC Centre of Excellence in Exciton Science, School of Physics, UNSW Sydney, NSW 2052, Australia*

<sup>¶</sup>*School of Photovoltaic and Renewable Energy Engineering, UNSW Sydney, NSW 2052, Australia*

E-mail: [timothy.schmidt@unsw.edu.au](mailto:timothy.schmidt@unsw.edu.au)

## X-ray diffraction

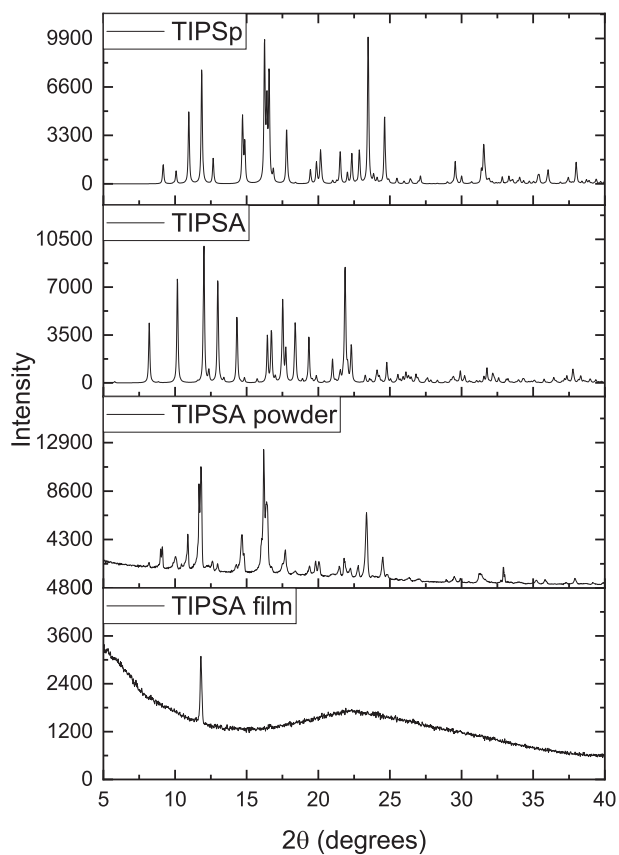


Figure S1: X-ray diffraction of TIPS-Ac films compared to TIPS-Ac powder and the two polymorphs, TIPSp (CCD deposition no. 1962254)<sup>S1</sup> and TIPSA (CCD deposition no. 962668),<sup>S2</sup> reported in the Cambridge crystal database.

## Photoluminescence

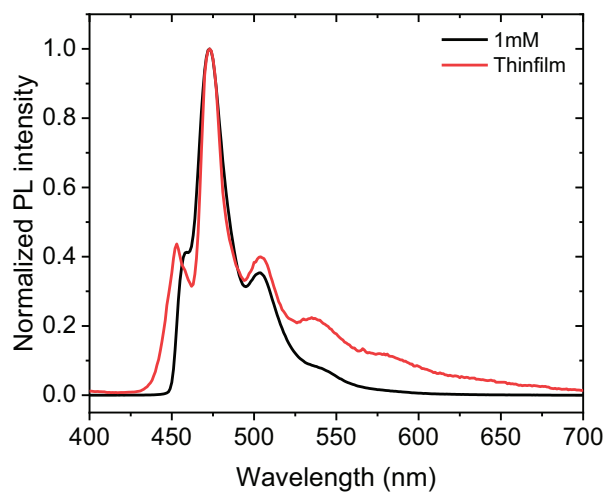


Figure S2: Steady state PL of thin-film TIPS-Ac compared to a 1 mM solution. Samples were excited at 355 nm. Steady-state PL measurements were taken with an Edinburgh Instruments FS5 spectrofluorometer.

## Additional transient absorbance data

### Transient absorbance 1 mM solution

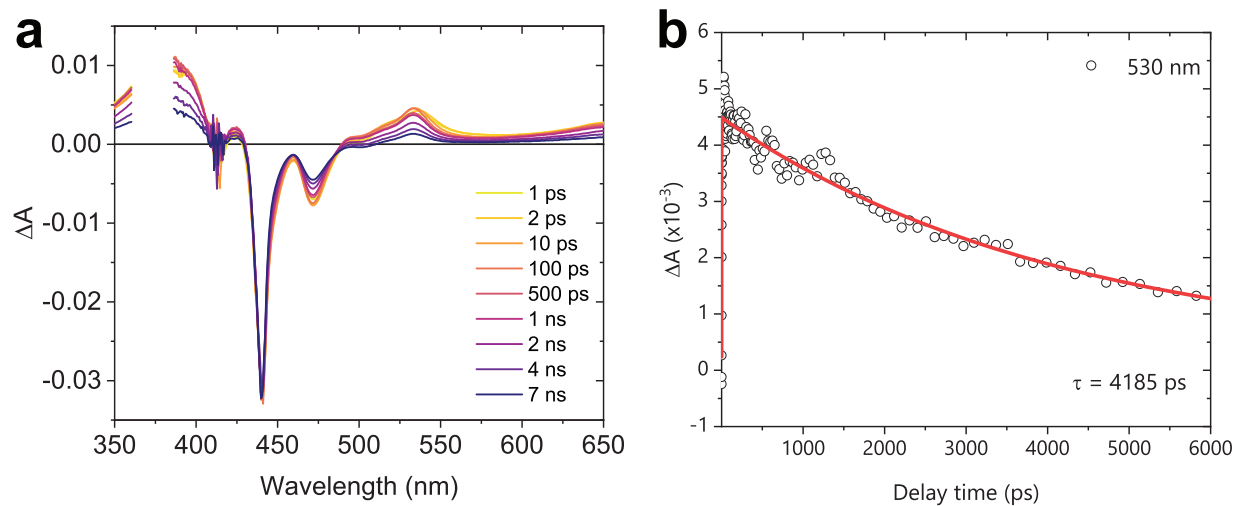


Figure S3: Transient absorption of 1mM TIPS-Ac in toluene. Excited at 380 nm ( $51 \mu\text{J cm}^{-2}$ , 1 kHz, 100 fs duration pulses). (b) Initial decay fitted to a monoexponential with the time constant of  $4185 \pm 500$  ps.

## Triexponential global fit

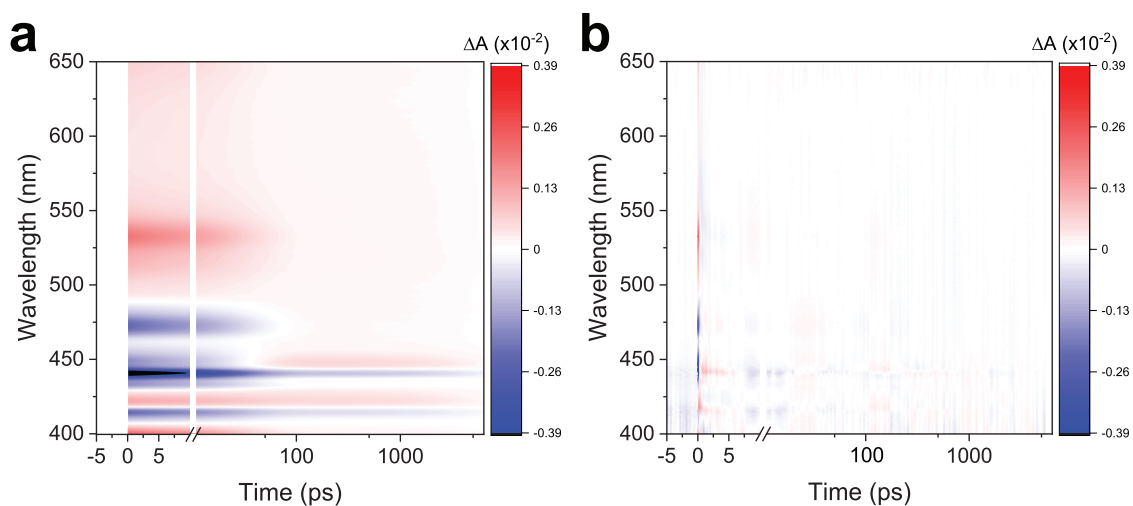


Figure S4: TA data of the thin films (a) fitted with a triexponential using the least squares method and the resulting residuals (b). This fit is reported in the main text with the following time constants:  $\tau_1 = 14 \pm 1$  ps,  $\tau_2 = 115 \pm 9$  ps,  $\tau_3 > 7$  ns .

## Biexponential global fit

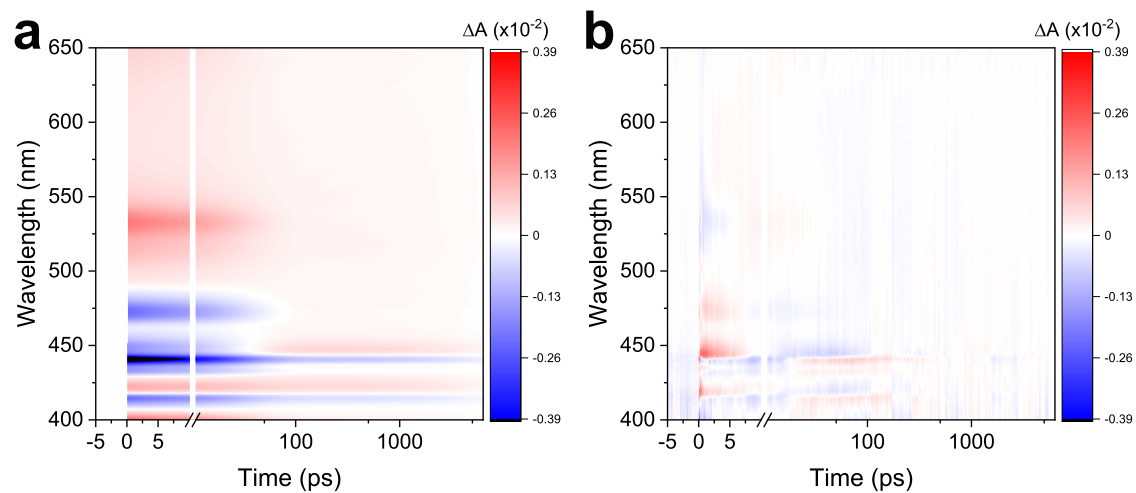


Figure S5: TA data of the thin films (a) fitted with a bi-exponential using the least squares method and the resulting residuals (b). This fit shows that a bi-exponential does not accurately represent the TA data

## Triplet lifetime

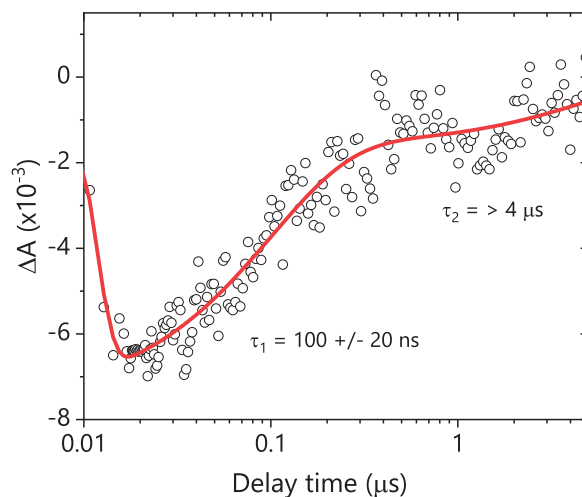


Figure S6: Kinetics of the long-time spectrum probed at the 442 nm GSB. The red line is a mono-exponential fit with the fitting result of  $\tau_1 = 100 \pm 20 \text{ ns}$  and  $\tau_2 > 4 \mu\text{s}$

## SF-yield calculations

The ground state bleach (GSB) represents a depletion of the ground state absorption as chromophores are excited by the pump pulse. As chromophores return to the ground state the GSB recovers. However, if SF takes place these chromophores will end up in the triplet state and will not return to the ground state within the temporal range of the experiment (7 ns) resulting in persistence of the GSB. Therefore, the SF-yield can be calculated by estimating the contribution of the GSB to the transient spectrum. An estimation of the GSB contribution is obtained by fitting a negative-going linear absorption spectrum to the transient spectrum (Figure S7). To obtain a reasonable fit the excited state absorptions (ESA) are modelled with a single gaussian at early times and two gaussian's at latter times. The values in Figure S7 are the GSB contributions. By dividing the latter time contributions (Figure S7 c, f) by the early time (Figure S7 a, d) a SF-yield estimation is made. This process is carried out for both the species associated spectra and the raw TA spectrum, the resulting yields are 23% and 19% respectively. Thus, the upper limit for SF-yield in these films is 19%.

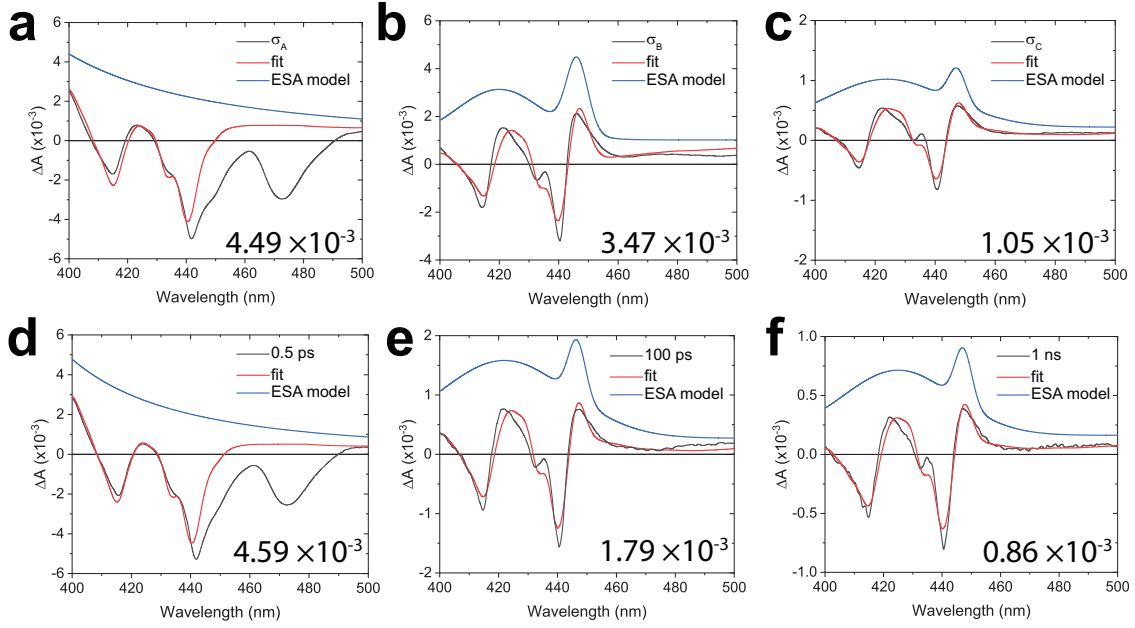


Figure S7: Spectral fitting of the transient absorption data for SF-yield calculations. The numbers inset represent the relative contribution of the ground state bleach to the transient spectrum. (a), (b) and (c) are model fits of the species associated spectra  $\sigma_A$ ,  $\sigma_B$  and  $\sigma_C$  respectively. (d), (e) and (f) are the model fits of the raw TA data at 0.5 ps, 100 ps and 1 ns respectively.

## Deriving the decay and species associated spectra

For well-separated time-scales, a kinetic scheme written as



will have

$$[a]_t = [a]_0 (x \exp(-t/\tau_2) + (1 - x) \exp(-t/\tau_1)) \quad (2)$$

and

$$[b]_t = [a]_0 (1 - x) (\exp(-t/\tau_2) - \exp(-t/\tau_1)) \quad (3)$$

where  $\tau_1 = 1/(k_1 + k_{-1})$  and  $\tau_2 = 1/k_2$ . Species  $c$  is generated and then decays on a long time scale.

$$[c]_t = \Phi[a]_0 (\exp(-t/\tau_3) - \exp(-t/\tau_2)) \quad (4)$$

where we include a yield,  $\Phi$ .

The transient absorption spectrum  $\sigma(\lambda, t)$  can be generated by multiplying the concentrations by a molar absorbance  $\Delta\varepsilon(\lambda)l$ , where  $l$  is the sample thickness, and adding.

$$\begin{aligned} \sigma(\lambda, t) &= [a]_0 l (\Delta\varepsilon_a x \exp(-t/\tau_2) + \Delta\varepsilon_a (1-x) \exp(-t/\tau_1) \\ &\quad + (1-x) (\Delta\varepsilon_b \exp(-t/\tau_2) - \Delta\varepsilon_b \exp(-t/\tau_1)) \\ &\quad + \Phi (\Delta\varepsilon_c \exp(-t/\tau_3) - \Delta\varepsilon_c \exp(-t/\tau_2))) \end{aligned} \quad (5)$$

$$\begin{aligned} &= \sigma_a (x \exp(-t/\tau_2) + (1-x) \exp(-t/\tau_1)) \\ &\quad + \sigma_b (1-x) (\exp(-t/\tau_2) - \exp(-t/\tau_1)) \\ &\quad + \Phi \sigma_c (\exp(-t/\tau_3) - \exp(-t/\tau_2)) \end{aligned} \quad (6)$$

The decay-associated spectra are therefore

$$\sigma_1 = (1-x)\sigma_a - (1-x)\sigma_b \quad (7)$$

$$\sigma_2 = x\sigma_a + (1-x)\sigma_b - \Phi\sigma_c \quad (8)$$

$$\sigma_3 = \Phi\sigma_c \quad (9)$$

## Kinetic modeling of the magnetic photoluminescence

Figure S8 depicts the full kinetic model used in Figure 7. Note that Figure 7a and d depict a simplified version of the below model as different aspects of the model are investigated:

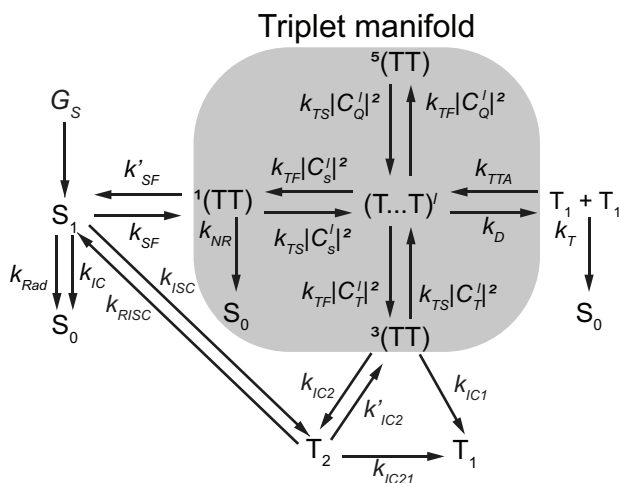


Figure S8: Modified Kinetic model from Clark and co-workers.<sup>S3</sup>

### Initial excited concentration

The initial excited population of the  $S_1$  state was calculated by first calculating the photon energy at 380 nm follows:

$$E_{380\text{ nm}} = \frac{hc}{\lambda} \quad (10)$$

where  $h$  is Planck constant,  $c$  the speed of light, and  $\lambda$  is 380 nm. Next, the absorbed photon density is calculated as follows:

$$\rho = \frac{\frac{f}{E_{380\text{ nm}}} \times (1 - 10^{-A_{380\text{ nm}}})}{\ell} \quad (11)$$

Where  $\ell$  is the thickness of the thin film which is measured as 200 nm,  $f$  is the fluence of the laser ( $15 \mu\text{Jcm}^{-2}$ ), and  $A_{380\text{ nm}}$  is the linear absorption at 380 nm. Finally, the concentration of excited molecules is calculated:

$$C = \frac{\rho \times 1000}{N_A} \quad (12)$$

The excited concentration of molecules is therefore 0.86 mM.

## Rate equations

The rate equations for the model represented in Figure S8 are described as follows

$$\frac{d[T_1]}{dt} = 2k_D \sum_{l=1}^9 (T \dots T)^l + k_{IC21}[T_2] + k_{IC1}|C_T^l|^2 [{}^3(TT)] - 2k'_{TTA}[T_1][T_1] - k_T[T_1] \quad (13)$$

$$\begin{aligned} \frac{d[T \dots T]^l}{dt} &= \frac{1}{9} k'_{TTA}[T_1][T_1] - k_D[(T \dots T)^l] - k_{TF}(|C_S^l|^2 + |C_T^l|^2 + |C_Q^l|^2) \\ &+ k_{TS}(|C_S^l|^2 [{}^1(TT)] + \sum_{m=x,y,z} |C_{Tm}^l|^2 [{}^3(TT)_m] + \sum_{m=x,y,z} |C_{Qm}^l|^2 [{}^5(TT)_m]) \end{aligned} \quad (14)$$

$$\frac{d[{}^5(TT)_m]}{dt} = 2k_{TF} \sum_{l=1}^9 |C_{Qm}^l|^2 [(T \dots T)^l] - k_{TS} \left( \sum_{l=1}^9 |C_{Qm}^l|^2 \right) [{}^5(TT)_m] \quad (15)$$

$$\begin{aligned} \frac{d[{}^3(TT)_m]}{dt} &= k_{TF} \sum_{l=1}^9 |C_{Tm}^l|^2 [(T \dots T)^l] - k_{TS} \left( \sum_{l=1}^9 |C_{Tm}^l|^2 \right) [{}^3(TT)] \\ &+ k'_{IC2} T_2 - (k_{IC1} + k_{IC2}) [{}^3(TT)] \end{aligned} \quad (16)$$

$$\frac{d[{}^1(TT)_m]}{dt} = k_{TF} \sum_{l=1}^9 |C_S^l|^2 [(T \dots T)^l] - k_{TS} \left( \sum_{l=1}^9 |C_S^l|^2 \right) [{}^1(TT)_m] + k_{SF}[S_1] - (k'_{SF} - k_{NR}) [{}^1(TT)] \quad (17)$$

$$\frac{d[(S)_1]}{dt} = G_s + k_{RISC}[T_2] + k'_{SF}[{}^1(TT)] - (k_{NR} + k_{SF} + k_{rad} + k_{ISC} + k_{IC})[S_1] \quad (18)$$

$$\frac{d[(T)_2]}{dt} = k_{IC2} \sum_{m=x,y,z} |C_T^l|^2 [{}^3(TT)_m] + k_{ISC}[S_1] - (k'_{IC2} + k_{RISC} + k_{IC21})[T_2] \quad (19)$$

The character of the singlet eigenstate is represented as:<sup>S4</sup>

$$|C_S^l|^2 = |\langle S|\psi_l\rangle|^2 \quad (20)$$

the triplet character as:<sup>S5</sup>

$$|C_T^l|^2 = \sum_{m=x,y,z} |\langle T_m|\psi_l\rangle|^2 \quad (21)$$

And the quintet character as:

$$|C_Q^l|^2 = \sum_{m=a,b,x,y,z} |\langle Q_m|\psi_l\rangle|^2 \quad (22)$$

## Singlet character of the triplet-pair eigenstates

To calculate the singlet character of the triplet-pair eigenstates, we use the following form for the triplet-pair spin Hamiltonian:

$$H_{TT}(B) = H_{zfs} + H_{zee}(B) + H_{exc} \quad (23)$$

consisting of the zero-field splitting, Zeeman splitting, and inter-triplet exchange coupling terms. For each value of the magnetic field, we numerically diagonalise  $H_{TT}$  to find its eigenstates, and compute

$$\langle {}^1TT|e_i\rangle, \quad i = 1, 2, \dots, 9 \quad (24)$$

for each eigenstate  $|e_i\rangle$ , where  $|{}^1TT\rangle$  is the unique eigenstate of the triplet-pair  $S^2$  matrix with

eigenvalue 0. The ZFS parameters of TIPS-anthracene ( $D = 2063\text{MHz}$ ,  $E = -243\text{MHz}$ ) were estimated using those of an ordinary anthracene model.<sup>S6</sup> One anthracene molecule of the pair has its ZFS tensor rotated according to Euler angles  $\alpha = 0^\circ$ ,  $\beta = 12.39^\circ$ ,  $\gamma = 0^\circ$ , in accordance with the nearly coplanar nearest-neighbour pair identified from the crystal structure in CCDC file number 962668.

## Rates from model

The free energy ( $G$ ) for  $S_1$  is set at 0 and  $-K_B T \ln(5.25)$  for  ${}^1(\text{TT})$ ,  ${}^l(\text{T...T})$ , and  $T_1$ . Where 5.25 is the calculated equilibrium constant from the TA.

Table S1: Rates applied to the model

Rate	Value ( $\text{s}^{-1}$ )	Notes
$k_{rad}$	$1 \times 10^8$	
$k_T$	$2.5 \times 10^5$	Approximated from $T_1$ lifetime (Figure S6)
$k'_{SF}$	$3.2 \times 10^9$	$k_{SF} \times e^{(G_1(\text{TT})-G_S)}$
$k_{SF}$	$1.7 \times 10^{10}$	
$k_{TF}$	$1 \times 10^{10}$	Lower bound of triplet hopping rate <sup>S3,S7</sup>
$k_{TS}$	$1 \times 10^{10}$	$k'_{TF} \times e^{(G_{TT}-G_{(T...T)^l})}$
$k_D$	Varied	See Fig. 7b
$k_{TTA}$	Varied	Scales linearly with $k_D$ (Fig. 7b)
$k_{IC21}$	$1 \times 10^{12}$	
$k_{IC}$	varied	$6.7 \times 10^{10} - k_{ISC} - k_{SF} - k'_{SF} - k_{rad}$
$k_{IC2}$	$1 \times 10^9$	
$k'_{IC2}$	$1 \times 10^9$	$k'_{IC2} \times e^{(G_{T_2}-G_{1TT})}$
$k_{IC1}$	$1 \times 10^9$	
$k_{NR}$	$9 \times 10^9$	
$k_{RISC}$	Varied	See Fig. 7e
$k_{ISC}$	Varied	See Fig. 7e

## References

- (S1) Moliterni, A.; Altamura, D.; Lassandro, R.; Olieric, V.; Ferri, G.; Cardarelli, F.; Cam-  
poseo, A.; Pisignano, D.; Anthony, J. E.; Giannini, C. Synthesis, crystal structure, polymor-  
phism and microscopic luminescence properties of anthracene derivative compounds. *Acta*  
*Crystallographica Section B: Structural Science, Crystal Engineering and Materials* **2020**,  
76, 427–435.
- (S2) Anthony, J. E.; Parkin, S. *CSD Communication* **2016**,
- (S3) Bossanyi, D. G.; Sasaki, Y.; Wang, S.; Chekulaev, D.; Kimizuka, N.; Yanai, N.; Clark, J. Spin  
Statistics for Triplet–Triplet Annihilation Upconversion: Exchange Coupling, Intermolecular  
Orientation, and Reverse Intersystem Crossing. *JACS Au* **2021**, 1, 2188–2201.
- (S4) Johnson, R. C.; Merrifield, R. E. Effects of Magnetic Fields on the Mutual Annihilation of  
Triplet Excitons in Anthracene Crystals. *Physical Review B* **1970**, 1, 896–902.
- (S5) Mezyk, J.; Tubino, R.; Monguzzi, A.; Mech, A.; Meinardi, F. Effect of an External Magnetic  
Field on the Up-Conversion Photoluminescence of Organic Films: The Role of Disorder in  
Triplet-Triplet Annihilation. *Physical Review Letters* **2009**, 102, 087404.
- (S6) Haarer, D.; Schmid, D.; Wolf, H. C. Elektronenspin-Resonanz von Triplett-Exzitonen in An-  
thrazen. *physica status solidi (b)* **1967**, 23, 633–638.
- (S7) Biaggio, I.; Irkhin, P. Extremely efficient exciton fission and fusion and its dominant con-  
tribution to the photoluminescence yield in rubrene single crystals. *Applied Physics Letters*  
**2013**, 103, 263301.